CONSTRUCTION STATUS OF THE SUPERCONDUCTING LINAC AT THE RIKEN RADIOACTIVE ISOTOPE BEAM FACILITY

N. Sakamoto*, M. Dantsuka, H. Imao, O. Kamigaito, K. Kusaka, H. Okuno, K. Ozeki, K. Suda,
T. Watanabe, Y. Watanabe, K. Yamada, RIKEN Nishina Center, Saitama, Japan
E. Kako, H. Nakai, H. Sakai, K. Umemori, KEK, Ibaraki, Japan
H. Hara, K. Miyamoto, K. Sennyu, T. Yanagisawa,
Mitsubishi Heavy Industries Machinery Systems, Ltd. (MHI-MS), Kobe, Japan

Abstract

The RIKEN Heavy-Ion Linac (RILAC) is undergoing an upgrade to allow it to further investigate super-heavy elements. In this project, a new superconducting (SC) electron cyclotron resonance ion source and SC booster linac are being developed and constructed. The SC Linac consists of 10 TEM quarter-wavelength resonators that are operated at 73 MHz and contained in three cryomodules. The design and construction status of the Superconducting RILAC, including the medium-energy beam transport line, are given in this paper.

INTRODUCTION

The mission of the RIKEN Radioactive Isotope Beam Factory (RIBF) [1, 2] is to improve our understanding of the mechanism of synthesis of elements in the universe via experiments using intense heavy-ion beams. At the RIBF, heavy-ion beams with various energies are available from sub-coulomb energy levels for fusion reactions to intermediate energy levels for radioisotope beam production using fission reactions. Beams of ion species ranging from hydrogen to uranium are accelerated in accordance with experimental requirements.

The most important upgrades are designed to increase the beam intensity and acceleration voltage in order to synthesize super-heavy elements, because its reaction cross section is estimated to be as small as a femtobarn. The original RILAC [3] consists of six drift-tube-linac (DTL) tanks that are frequency-tunable from 17 to 45 MHz, and can accelerate heavy-ions to 2.9 MeV/u at 37.75 MHz. The new element Nh was synthesized by bombarding a ^{209}Bi target with an intense ^{70}Zn^{14+} beam with an energy of 5 MeV/u [4] accelerated by the RILAC, which was upgraded by adding a booster linac [5] comprising six DTLs. The first two DTLs of the booster, A1 and A2, are equipped with short-plate frequency tuning systems to have a frequency range from 36 to 76 MHz, which will expand the energy range of the beam injected to the RIKEN Ring Cyclotron, while the latter four DTLs have a fixed frequency.

The Superconducting RILAC (SRILAC) was proposed [6] in order to allow further experiments on super-heavy element synthesis. To preserve the versatility of the beams that are utilized for coupled operation of the RILAC and RRC, it was decided to upgrade the RILAC by replacing the latter 4 DTLs

---

* nsakamot@ribf.riken.jp

of the booster linac, which are fixed-frequency cavities, with a SC linac. The goals of the upgrade are listed in Table 1.

Table 1: Specifications of RILAC Before and After Upgrade

Upgrade	Before	After
No. of tanks	12 DTLs	8 DTLs, 3 CMs
Freq. (MHz)	37.75/75.5	36.5*/73.0
Total Acc. V (MV)	25 (A/q = 5)	39 (A/q = 6)

* 36.5 MHz is the fundamental frequency for the RF system of the RIBF accelerators.

The design of the SRILAC is based on the idea of increasing the intensity of the uranium beams and accelerating them to up to 11 MeV/u [7,8]. The original design of the SRILAC consists of 14 cryomodules (CMs), and each CM accommodates four quarter-wavelength resonators QWRs. The QWRs are optimized for a beta of 0.08 and an energy of about 3 MeV/um, which matches the energy of the beams provided by the RILAC. As shown in Fig. 1, the SRILAC consists of three CMs–CM1, CM2, and CM3–with a room-temperature medium-energy beam transport (MEBT) between them. The CMs do not contain superconducting magnets. The design of the CMs is a modification of a prototype CM developed at RIKEN [9–11] as a part of the ImPACT Program [12]. For the MEBT, a newly designed beam energy position monitor will be employed instead of traditional wire scanners. Since the SRILAC will be installed in the existing facility, it is important to have an isolation system to prevent contamination of the SC parts.
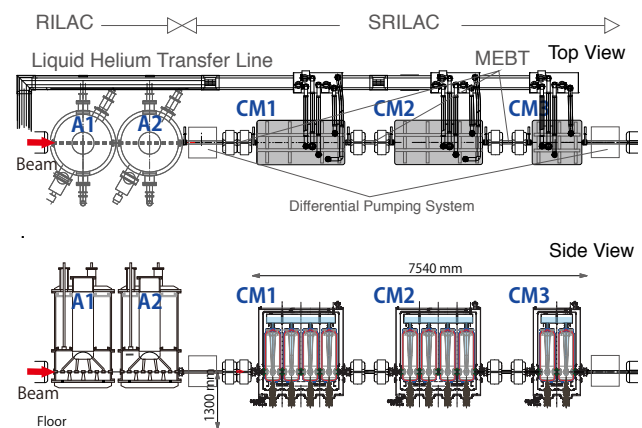

Figure 1: Layout of the Superconducting RILAC.

SUPERCONDUCTING UPGRADES TO THE RILAC

SC Linac

The SRILAC is designed to operate in continuous wave (c.w.) mode. Operational parameters of the CMs are listed in Table 2. The gap length of the cavity is optimized for

Table 2: Operational Parameters of the SRILAC

Parameter	Value
Frequency (MHz)	73.0 (c.w.)
E_{inj} (MeV/u)	3.6
E_{ext} (MeV/u)	6.5 for A/q = 6
Number of cavities	10
Cavity type	TEM, $\lambda/4$
Max. gap voltage (MV)	1.2
Synchronous phase (°)	–25
Max. acc. gradient (MV/m)	6.8
Target Q_0	1×10^9 @ E_{acc} = 6.8 MV/m
Beam current (μA)	≤100
Q_{ext}	1–4.5×10^6
Amplifier output (kW)	7.5

β=0.08 particles with a transit time factor (TTF) of 0.9. The gap voltage is 1.2 MV, which corresponds to an acceleration gradient E_{acc} of 6.8 MV/m with a synchronous phase of -25°. The SRILAC is based on 10 superconducting QWRs.

The cavities are made from pure Nb sheets with a residual resistivity ratio of 250, and their inner surfaces are processed by buffered chemical polishing (BCP). Each bulk Nb cavity is contained within a helium vessel made of pure Ti. The operating temperature is 4.5 K and the target Q_0 is 1×10^9 at an E_{acc} of 6.8 MV/m. The maximum current in the heavy-ion beams is 100 μA for the super-heavy element synthesis experiments; therefore, beam loading is negligible. The power coupler is designed with a tunable coupling so that a Q_{ext} range from 1×10^6 to 4.5×10^6 can be achieved by changing the insertion distance of its antenna. Q_{ext} was chosen to be as small as 10^6 due to detuning of the resonance frequency of each QWR. To have an operational bandwidth of ±60 Hz, an output power of 7.5 kW is required for the RF amplifiers.

Due to the vertical asymmetry of the QWR structure, the accelerated beams are kicked downward by the RF magnetic field. To counteract this steering effect, the faces of drift tubes are tilted at an angle of ±2.3° [8,13]. This modification of the drift tube shape produces a vertical component in the electric field to correct the downward steering of the accelerated beams.

SC Cavity

The SC cavity design, as shown in Fig. 2, was modified from the first prototype cavity to reduce the cost. The number of ports was reduced from nine to six, and now there are two rinsing ports, two beam ports, a coupler (vacuum) port, and a pickup antenna port. The geometry of the cavity was optimized using the 3D simulation package CST Microwave Studio [14], as shown in Fig. 2. Characteristics of the optimized QWR are summarized in Table 3. The conical shape of the stem improves RF performance to reduce the peak magnetic field and increase the rigidity against pendulum vibration.
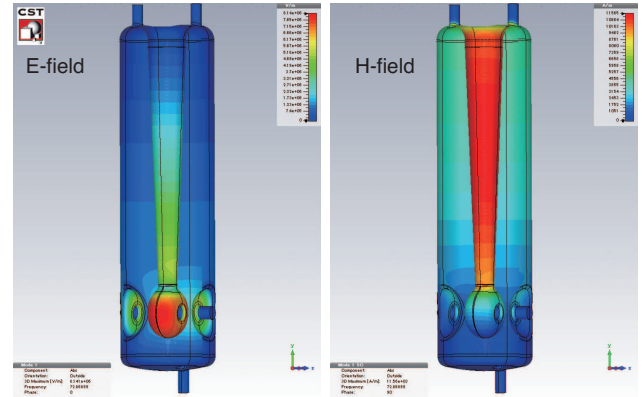

Figure 2: Contour plots of electric (E) and magnetic (H) fields in SC cavity.

Table 3: Characteristics of QWR for SRILAC

Parameter	Value
Frequency at 4.5 K (MHz)	73.0
β_{opt}	0.08
E_{peak}/E_{acc}	6.0
B_{peak}/E_{acc} ($\frac{mT}{MV/m}$)	9.5
R_{sh}/Q_0 for β_{opt} (Ω)	578
G (Ω)	22.6
P_0 (W)	4.0
Inner diameter (mm)	300
Height (mm)	1,100
Beam tube aperture diameter (mm)	40.0

A schematic of the QWR mechanical systems is shown in Fig. 3. Because the operating temperature is 4 K, boiling helium bubbles may induce mechanical vibration in the stem. Thus, a mechanical damper is used to mitigate the effect of microphonics. This damper is a 90 cm cylindrical rod inserted into the stem to attenuate the vibration. Extensive mechanical analysis of the liquid helium pressure was also performed. Dynamic tuning is realized by pressing beam ports. The shift in frequency by the tuner is limited within –20 kHz because the maximum stress on the pure Nb part cannot exceed 90 MPa, as required by regulations for high-pressure safety in Japan.

After validation of prototype cavity, six bulk SC cavities have been fabricated and processed with inner surface treatment to date, and four more are being fabricated. All cavities are carefully inspected after every processing step, including welding, BCP, high-pressure rinsing, annealing,

Figure 3: QWR for SRILAC.

Figure 4: Photos of SRF infrastructure: (1) ISO Class 1 horizontal-flow clean room looking downstream, (2) Coupler test stand in clean room, (3) View of vertical test booth, and (4) Installation of bulk superconducting cavity into the test cryostat for vertical testing (VT).
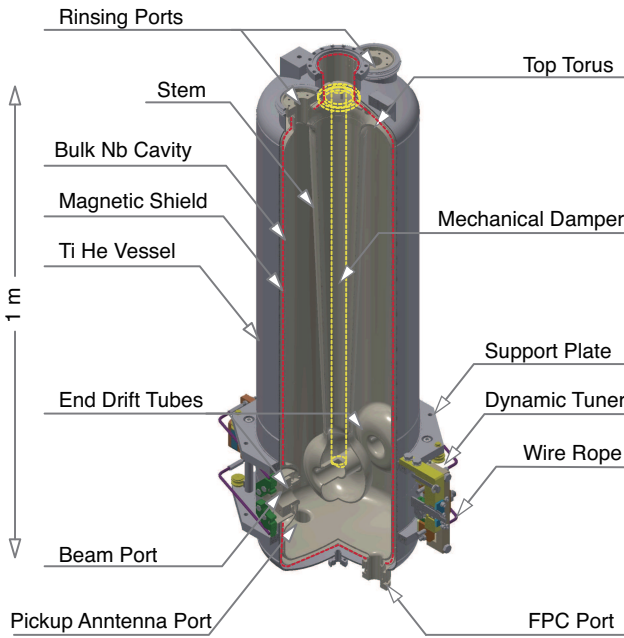
venting, and cooling. In addition, during these processing steps, the eigenmode frequency of every cavity is measured and adjusted to maintain this frequency so as to be finally within the range of the dynamic tuner at 4K.

The SRF infrastructure for vertical testing and cleanroom work was constructed at the RIKEN campus [9, 15]. Photographs of the infrastructures are shown in Fig. 4. The constructed horizontal-flow clean room meets International Standards Organization (ISO) class 1 [15] and is equipped with a washing booth with an ultrapure water system. In Fig. 5, Q_0 values are plotted as a function of E_{acc} after cooling down to 4.2 K for the prototype cavity and six delivered cavities. Measurements were performed with a maximum E_{acc} of about 12 MV/m to avoid a degradation of cavity performance due to spark discharge. Note that the maximum value of E_{acc} in the measurement was not limited by field emission or quenching. The Q_0 performance of all cavities shows similar behavior and exceeds the goal of 1×10^9 at E_{acc} of 6.8 MV/m at 4.2 K.

At an E_{acc} of 0.4 and 0.8 MV/m, sudden Q_0 drop due to multipacting phenomena, that is, when RF power is consumed by electron emission, were observed as indicated in Fig. 5. It was found that multipacting at 0.4 MV/m occurred near the surface, where the electric field has a peak value (see Fig. 2), while multipacting at 0.8 MV/m occurred near the top surface of the torus [9]. Occasionally, heavy multipacting at E_{acc} of less than 0.1 MV/m was observed. Empirically, effective conditioning could be performed with c.w. RF power of more than 50 W with an over-coupled input-power antenna position.

The effect of the mechanical damper was also investigated. A power spectrum analysis of the time-series data for frequency during verification testing (VT) was sampled at an interval of 1 ms. The power spectrum with and without a
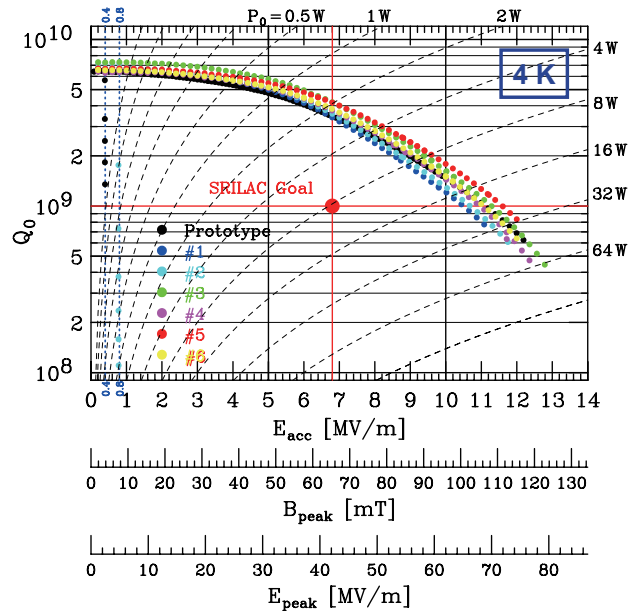
Figure 5: Cavity performance validation. The Q_0 values of bulk cavities measured at 4.2 K are plotted as a function of E_{acc}, E_{peak}, and B_{peak}. Dashed lines indicate lines of constant power dissipation.

damper are plotted in Fig. 6 as green and blue curves, respectively. Three peaks appeared at 24, 50, and 71 Hz for #6 without a damper (green curve in Fig. 6). In contrast, for #5 with a damper, the two peaks at 24 and 71 Hz disappeared and the frequency of the second peak at 50 Hz decreased. The effectiveness of the mechanical damper is still under investigation.
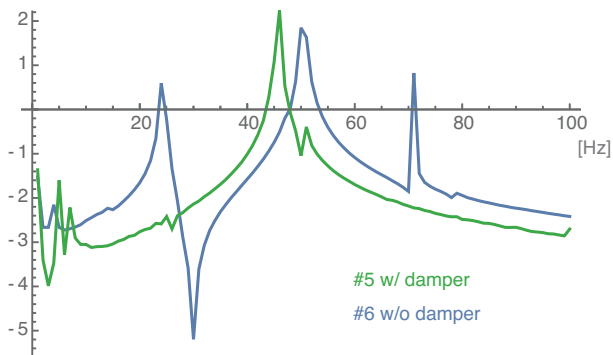
Figure 6: Analysis of time-series data for frequency shift.

After validation of the bulk cavities, helium jackets and magnetic shields made from Mu-Metal sheets will be installed between the cavity and the helium vessel. Before proceeding to cold mass assembly, vertical testing will be performed again to confirm the cavity performance for Q_0, that a no-field-emission condition is maintained, and that the eigenmode frequency does not change. If the eigenmode frequency is not in the tuning range of the dynamic tuner, frequency tuning by differential BCP, for example, will be required.

Meanwhile, the FPCs shown in Fig. 7 with a single-window structure were conditioned using a conditioning resonator [16]. A pair of FPCs were conditioned with 5 kW of c.w. RF power, as shown in Fig. 4(2). The ceramic window is located in the room-temperature part of the coupler. Cleaning of the coupler, assembling the test resonator, and RF conditioning were performed in the ISO class 1 clean room.
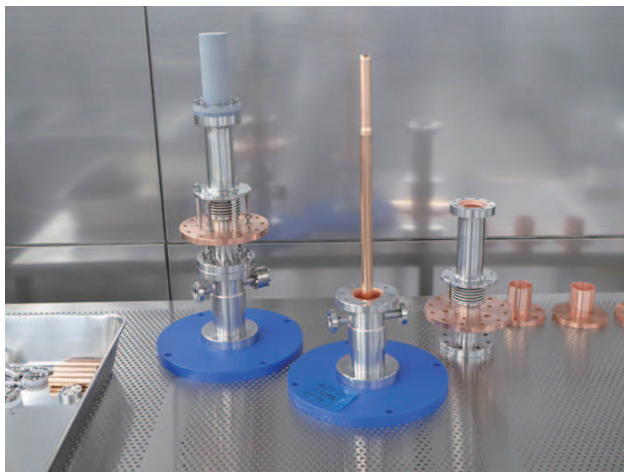

Figure 7: Photo of fundamental power couplers.

The dynamic tuner is attached to the support plates (see Fig. 3), which are welded to the helium vessel. The tuner driven by a stepping motor reduces the frequency in the cavity by tightening the surrounding wires. The driving structure was modified from the original design of the prototype to improve the capability to counteract mechanical losses due to the 4-K temperature.

Cryomodules

The SRILAC CM design is based on the first prototype cryomodules [9]. A schematic of cryomodules CM1 and CM2 is shown in Fig. 8. CM3, which contains two QWRs, is generally based on the same design as CM1 and CM2. The cold mass, which consists of a cavity, magnetic shield, helium vessel, FPC, and dynamic tuner, is supported by pillars made of G10 from the bottom base plate; that is, the CM is not a traditional top-loading type. Each cold mass is connected with beam bellows to separate the cavity vacuum from the insulation vacuum.
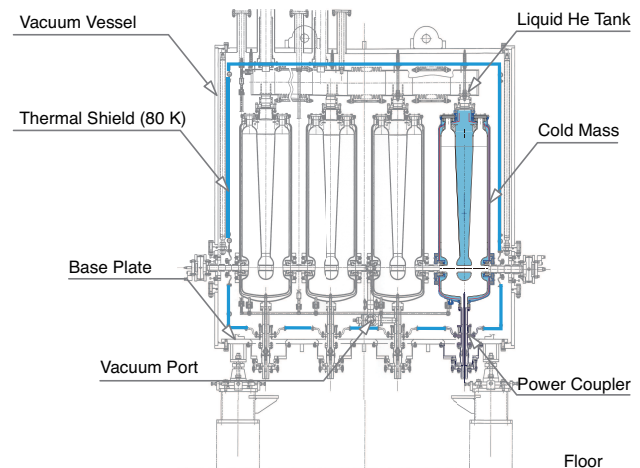

Figure 8: Side views of CM1 and CM2.

The cold mass is cooled by 4-K liquid helium provided by a liquid helium cryogenic system using a HELIAL MF refrigerator (Air Liquide). Thermal anchors connect the support pillars to the 80-K thermal shields, which are cooled by liquid nitrogen. The 80-K thermal shields also provide thermal anchors for the FPCs and beam pipes. No superconducting magnet is installed in the CMs.

Another major modification concerns the magnetic shielding. As mentioned above, the Mu-Metal magnetic shields, indicated by red dashed lines in Fig. 3, are housed inside the helium vessel surrounding the bulk cavity (Fig. 9(1)). This design enables the minimization of the effect of possible magnetization of cold mass components by placing them outside the shields. For example ball bearings are used for the dynamic tuners. Moreover, this arrangement makes it much easier to assemble and handle the cold mass. In addition to the local shielding, the vacuum vessel is made of carbon steel instead of the stainless steel employed to shield the external magnetic field.

Pre-assembly of the CMs is scheduled for October at Mitsubishi Heavy Industries Machinery Systems, Mihara. Full CM assembly will take place in this year at RIKEN, Wako.

OTHER ISSUES

MEBT and Beam Monitor

The MEBT, which connects the CMs, as shown in Fig. 1, has the functions of maintaining the vacuum, transversely

Figure 9: Photos of jacketed cavity: (1) Pre-assembly and (2) Assembly #3 prepared for VT

Figure 10: Schematic of compact differential pumping system.

focusing the beam, and performing beam diagnostics. For beam transport, room-temperature quadrupole magnets, including a function of horizontal and vertical steering, are used. Instead of traditional beam diagnostic devices, such as wire scanners and Faraday cups, beam energy position monitors are employed. These monitors are intended to measure not only the energy and position but also the size of the beam. Since beam measurement is non-destructive, ideally there is neither outgassing nor spattering to produce particulates in the high-vacuum sections. Development of the new beam diagnostics for SRILAC is underway in cooperation with the Beam Diagnostics Group of J-PARC.

Differential Pumping System

One of the most important issues in designing the beam transport line is how to prevent contamination of SC cavities by particulates transported from the room temperature section by gas flow due to the vacuum pressure gradient. While the vacuum pressure level of the SC part reached as high as 10×10^{-8} Pa, the vacuum pressure in the RILAC, designed and built more than 37 years ago (first beam in 1981), is 1×10^{-5} Pa to 1×10^{-6} Pa. To connect the different vacuum level parts and prevent gas flow into the high-vacuum section, a non-evaporable-getter-based differential pumping system was proposed [17]. A schematic of the differential pumping system is shown in Fig. 10. This system reduces pressure from the vacuum of the existing beam line of RILAC to the ultra-high vacuum in the CMs. It has a very compact size of 750 mm. Cleaning and assembly of the parts are underway.

Outlook

To date, six bulk cavities have been tested, and the jacketing process for them is underway. It is planned to have a VT with one more bulk cavity. The other three cavities are going to be jacketed without a VT procedure. Full assembly of the CM will be finished in the first quarter of 2019, and in-
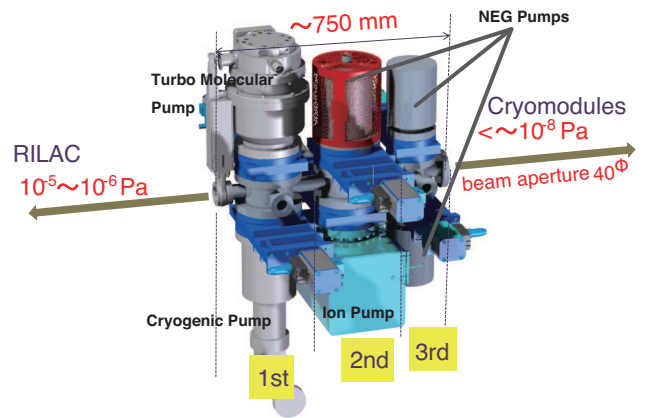
stallation in the accelerator building is scheduled for March 2019. After installing the MEBT, including the differential pumping systems, cooling and RF testing will be performed during the second quarter of 2019 with the aim of full beam commissioning in the third quarter of 2019.

ACKNOWLEDGMENTS

REFERENCES

[1] Y. Yano *et al.*, Nucl. Instrum. Methods, vol. B261, p. 1009, 1984.

[2] H. Okuno *et al.*, Prog. Theor. Exp. Phys., vol. 2012, p. 03C002, 2012.

[3] M. Odera *et al.*, Nucl. Instrum. Methods , vol. A227, p. 187(1984).

[4] K. Morita *et al.*, JPSJ, vol. 73, p. 2593, 2004.

[5] O. Kamigaito *et al.*, Rev. Sci. Instrum., vol. 76, p. 013306, 2005.

[6] O. Kamigaito *et al.*, "Present Status and Future Plan of RIKEN RI Beam Factory", in *Proc. IPAC'6*, Busan, Koreas, May 2016, paper, TUPMR022, p. 1281.

[7] K. Yamada *et al.*, "Conceptual Design of SC Linac of RIBF Upgrade Plan", in *Proc. SRF'13*, Paris, France, Sep. 2013, paper MOP021, p. 137.

[8] N. Sakamoto *et al.*, " Design Studies for Quarter-wave Resonators and Cryomodules for the RIKEN SC-Linac", in *Proc. SRF'15*, Whistler, BC, Canada, Sep. 2015, paper WEBA06, p. 976.

[9] N. Sakamoto *et al.*, "Construction and Performance Tests of Prototype Quarter-wave Resonator and its Cryomodule at

RIKEN", in Proc. SRF'17, Lanzhou, China, Jul. 2015, paper WEYA06, p. 681.

[10] T. Ozeki *et al*. "Cryomodule and power coupler for RIKEN Superconducting QWR", in *Proc. LINAC'16*, East Lansing, MI, USA, Sep. 2016, paper TUPLR061, p. 598.

[11] K. Yamada *et al*., "First Vertical Test of Superconducting QWR Prototype at RIKEN", in *Proc. LINAC'16*, East Lansing, MI, USA, Sep. 2016, paper THPLR040, p. 939.

[12] http://www.jst.go.jp/impact/en/program/08.html

[13] P. N. Ostroumov and K.W. Shepard, *Phys. Rev. ST. Accel. Beams*, vol. 4, p. 110101, 2001.

[14] http://www.cst.com

[15] A. Miyamoto *et al*., "MHI's Production Activities of Superconducting Cavity", in *Proc. SRF'15*, Whistler, BC, Canada, Sep. 2015, paper THPB029, p. 1141.

[16] K. Ozeki *et al*., "Cryomodule and Power Coupler for RIKEN Superconducting QWR", in *Proc. LINAC'16*, East Lansing, MI, USA, Sep. 2016, paper TUPLR061, p. 598.

[17] H. Imao, "NEG-based differential pumping system for SRILAC at RIBF" TTC meeting, Wako, Japan, Jun. 2018, https://indico.desy.de/indico/event/20010/session/21/contribution/106